# 1 Supplementary material: Tested aberration configurations

**Table 1** Summary of aberration configurations experimentally tested. For a given configuration, the changed family of aberration value is shown in blue. The coefficient $a_1$, $a_2$, ..., $a_{12}$ stand for defocus, astigmatism 0 °and 45 °, vertical coma, horizontal coma, spherical aberration, trefoil 0 °, trefoil 30 °, quadrafoil 0 °and 25 °, and second order astigmatism 0 °and 45 °. All the aberration coefficients presented in this table were averaged over 10 to 50 values depending on the number of shot conducted for each configurations.

| Configuration | Aberrations ($\lambda$ unit) | | | | | | | | | | | |
|---|---|---|---|---|---|---|---|---|---|---|---|---|
| Name | $a_1$ | $a_2$ | $a_3$ | $a_4$ | $a_5$ | $a_6$ | $a_7$ | $a_8$ | $a_9$ | $a_{10}$ | $a_{11}$ | $a_{12}$ |
| C-H-1 | -0.13 | -0.013 | -0.0018 | 0.058 | -0.0094 | -0.0058 | -0.0071 | -0.0069 | 0.0024 | -0.0008 | 0.0017 | -0.0044 |
| C-H-2 | -0.13 | -0.0078 | -0.0045 | 0.044 | -0.0087 | -0.0067 | -0.0065 | -0.0049 | 0.0007 | -0.0003 | 0.0005 | -0.0041 |
| C-HV-1 | -0.14 | -0.0061 | -0.001 | 0.059 | 0.051 | -0.0074 | -0.0089 | -0.0052 | 0.0027 | -0.0008 | 0.0016 | -0.0026 |
| C-HV-2 | -0.14 | -0.0017 | -0.006 | 0.045 | 0.038 | -0.0078 | -0.0090 | -0.0042 | 0.0023 | -0.0016 | 0.0003 | -0.002 |
| D | -0.05 | -0.012 | -0.0009 | -0.0011 | -0.01 | -0.0097 | -0.0054 | -0.005 | 0.0023 | 0.0008 | -0.0006 | -0.0011 |
| SA-1 | -0.17 | -0.008 | -0.01 | 0.003 | -0.012 | 0.047 | -0.0072 | -0.003 | 0.00025 | 0.007 | -0.0016 | -0.0009 |
| SA-2 | -0.17 | -0.007 | -0.009 | 0 | -0.01 | 0.032 | -0.006 | -0.0049 | 0.0018 | -0.0053 | -0.0007 | -0.0005 |
| A0H | -0.096 | 0.079 | -0.0025 | -0.0013 | -0.011 | -0.0091 | -0.0019 | -0.049 | 0.0020 | -0.0002 | -0.0025 | -0.0016 |
| A0M | -0.09 | 0.053 | -0.0021 | -0.0009 | -0.009 | -0.0096 | -0.0041 | -0.005 | 0.0022 | -0.0005 | -0.0022 | -0.0008 |
| A0 | -0.1 | 0.038 | -0.0043 | -0.0014 | -0.012 | -0.0089 | -0.0017 | -0.0043 | 0.0029 | -0.0006 | -0.0011 | -0.0016 |
| A-045-1 | -0.11 | 0.055 | 0.055 | -0.002 | -0.0088 | -0.0086 | -0.0011 | -0.0035 | 0.0013 | -0.0005 | -0.0022 | -0.0023 |
| A-045-2 | -0.19 | 0.035 | 0.021 | -0.004 | -0.009 | -0.0069 | -0.0033 | -0.003 | 0.0032 | -0.0048 | -0.0042 | -0.0037 |
| TTH | -0.16 | -0.0092 | -0.0004 | -0.0023 | -0.011 | -0.0077 | 0.055 | 0.055 | 0.006 | 0.0012 | -0.0005 | -0.001 |
| TTL | -0.16 | -0.0044 | -0.0046 | -0.0015 | -0.0089 | -0.0074 | 0.040 | 0.040 | 0.0053 | 0.0015 | -0.0016 | -0.0012 |
| Q-1 | -0.18 | -0.0079 | -0.037 | -0.0042 | -0.01 | -0.0096 | -0.0066 | 0.0022 | 0.043 | 0.036 | 0.0012 | -0.0025 |
| Q-2 | -0.17 | -0.0054 | -0.014 | -0.0021 | -0.012 | -0.012 | -0.0052 | 0.0039 | 0.054 | 0.049 | 0.0008 | -0.0025 |
| A2-0-1 | -0.0067 | -0.049 | -0.0061 | -0.0095 | -0.0026 | -0.015 | -0.0063 | 0.004 | 0.0049 | 0.0067 | 0.081 | -0.0005 |
| A2-0-2 | -0.17 | -0.028 | -0.013 | -0.0012 | -0.011 | -0.0086 | 0.0009 | -0.003 | -0.0037 | 0.0028 | 0.055 | -0.0029 |
| A2-0-3 | -0.18 | -0.033 | -0.0093 | -0.00037 | -0.014 | -0.0075 | 0.0005 | -0.003 | -0.0026 | 0.0004 | 0.044 | -0.0033 |
| A2-045-1 | -0.17 | -0.03 | -0.037 | 0.001 | -0.0071 | -0.01 | 0.0057 | 0.0016 | -0.0058 | 0.0096 | 0.052 | 0.051 |
| A2-045-2 | -0.2 | -0.03 | -0.02 | 0.001 | -0.001 | -0.0065 | 0.0026 | -0.0022 | -0.0037 | 0.0037 | 0.041 | 0.037 |
| TTA | -0.06 | -0.032 | -0.015 | -0.0088 | -0.0037 | -0.012 | 0.059 | 0.063 | 0.0035 | 0.0041 | 0.04 | -0.0022 |

Table 1 presents all the aberration configurations done during the experiment with their correspondent shot-to-shot variation in $\lambda$ units. To avoid over-complicating the results shown, not all tested configurations will be shown here. In Fig. 1 five consecutive shots on the beam monitor for five additional configurations are shown. Fig. 1a,b together with Fig. 6b (Main article), exhibit the sensitivity of the LWFA process to the astigmatism 0. Adding a 25 % more astigmatism 0 with respect to the A0 configuration (Table 1) makes the shape less stable in comparison and starts to display a multiple beam cluster to the around 25 mm to the left of the laser axis. Further increasing by 0.03 $\lambda$, vastly improves the apparition rate of the left cluster shape with the smudge on the right (Fig. 1b). The introduction of a 0.04 of second order astigmatism 0, creates on the beam monitor a faint circular pattern of radious ≈25 mm around a centered main beam (Fig. 1d). In some occasions (10 % of the shots) a secondary far beam appears on top of the circle. The configuration A2-045-1 is composed of 0.03 first order astigmatism 0 and 45 and 0.05 second order astigmatism 0 and 45 (Table 1, Fig. 1c). 65 % (15 % ) of the shots presents a nice beam shifted around 10 mm to the left to the laser axis with a weak circular pattern of 20 mm radious with a (two) bigger secondary beam on top. However 20 % of the shots something more akin to the multiple beams of the first order astigmatism without the weak circular pattern around it. Finally the ensemble of both trefoil aberrations (TTH) with a value of 0.55 (Table 1, Fig. 1d) generates a complex pattern with a beam slightly shifted from the laser axis and two weak beams aligned in a diagonal line, with an apparition rate of 75 %.

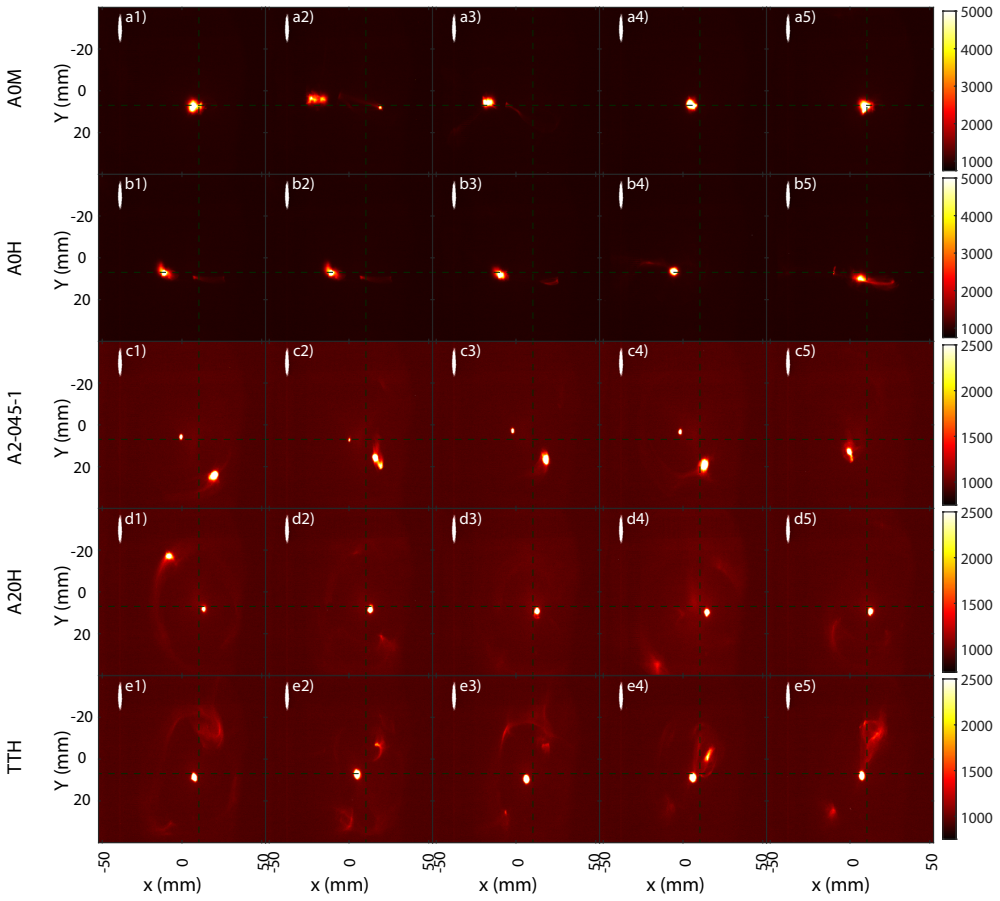


**Fig. 1** Five consecutive images of the electron beam transverse distribution recorded in the beam monitor for the aberration configurations a) A0M, b) A0H, c) A2-045-1, d) A20H and e) TTH (Table 1).

# References